Journal of Nuclear Materials 377 (2008) 141–146

Contents lists available at ScienceDirect

Journal of Nuclear Materials

journal homepage: www.elsevier.com/locate/jnucmat

Interaction of ⟨100⟩ and ½⟨111⟩ dislocation loops with point defects in ferritic alloys

D. Terentyev *, L. Malerba

SCK CEN, Nuclear Materials Science Institute, Boeretang 200, B-2400 Mol, Belgium

ARTICLE INFO

PACS:
75.50.Bb
61.82.Bg
61.72.Ji

ABSTRACT

The interaction between dislocation loops of interstitial nature with ½⟨111⟩ and ⟨100⟩ Burgers vectors and point defects in Fe has been studied molecular dynamics. Comparative calculations have been carried out using two interatomic potentials for pure Fe ([G.J. Ackland, M.I. Mendelev, D.J. Srolovitz, S. Han, A.V. Barashev, J. Phys.: Condens. Mater. 16 (2004) 1; S. Dudarev, P. Derlet, J. Phys.: Condens. Mater. 17 (2005) 7097]). The results of this study are range and energy of the interaction as functions of size and mutual position of defects. The applied potentials predict somewhat different strain field structure for ⟨100⟩ loops and therefore different lengths of interaction. However, both potentials suggest that, contrary to common belief, the distance of cluster-defect interaction within the glide prism of a ½⟨111⟩ cluster is significantly longer than that of a ⟨100⟩ cluster of similar size, in spite of the longer Burgers vector in the latter case.

1. Introduction

The presence of dislocation loops in pure Fe and ferritic alloys is an essential feature of radiation damage. Two types of dislocation loops are experimentally known to form in these metals, with different Burgers vectors, namely ½⟨111⟩ and ⟨100⟩ [3–5]. The rate of nucleation and growth of these loops defines the evolution of the microstructure in many respects and depends on their interaction (range and strength) with other radiation-induced defects, such as point defects and their small mobile clusters. It is believed that ½⟨111⟩ and ⟨100⟩ loops are sinks with different bias for point defects and that the magnitude of the bias increases with the length of Burgers vector [6,7]. This hypothesis was used to explain the low swelling in bcc Fe and ferritic steels (including high-Cr steels) [7,8]. However, not much is known about the interaction of different types of dislocation loops with point defects and their small clusters at the atomic scale level. It has been shown that self-interstitial atom (SIA) clusters of size up to a few nanometers cannot be described as perfect dislocation loops using an isotropic continuum approach [9], therefore an atomistic approach is required. The interaction of ½⟨111⟩ loops with point defects in bcc Fe has been studied already [9], but it is useful to revise the currently available results in the light of the recent advances in the development of interatomic empirical potentials (EPs) for Fe. On the other hand, no results on the interaction between ⟨100⟩ dislocation loops and point defects are so far available to our knowledge.

In this work a molecular static study of the interaction of ½⟨111⟩ and ⟨100⟩ dislocation loops with point defects in Fe is presented. Comparative calculations have been carried out using two EPs for pure Fe (Ackland, Mendelev et al. [1], and Dudarev and Derlet [2]). The main goal of this study is to estimate range and energy of the interaction as a function of size and mutual position of defects, which can be used in the parameterization of microstructure evolution models.

2. Method

Static calculations were used to estimate the interaction energy between SIA clusters containing up to 442 interstitials and point defects using the molecular dynamics code Dymoka [10]. Calculations have been carried out using two many-body interatomic EPs: one derived by Ackland, Mendelev et al. [1] (henceforth 'Mendelev's potential') and the other by Dudarev and Derlet [2] (henceforth 'Dudarev's potential'). The relaxation of the atomic configurations of interest has been performed at constant volume. The simulation boxes used in this type of calculations contained from 100 to 800 thousand atoms, thereby guaranteeing independence of the result from the box size. In all these static calculations the system was frozen at a temperature close to 0 K using a quench procedure to relax the atomic system at the equilibrium lattice constant. 3D periodic boundary conditions were employed. The results of test calculations of the cohesive energy, the equilibrium lattice constant at zero temperature and the converged formation energy of point defects are given in Table 1 for the mentioned EPs.

* Corresponding author. Tel.: +32 14 333197; fax: +32 14 321216.
E-mail address: dterenty@sckcen.be (D. Terentyev).

0022-3115/$ - see front matter © 2008 Elsevier B.V. All rights reserved.
doi:10.1016/j.jnucmat.2008.02.062

Table 1
Converged values of bulk properties, estimated in a box of 8192 atoms, using constant volume static relaxation

Potential	a_0 (Å)	Cohesive energy (eV)	Formation energies (eV)			
			Vacancy	⟨100⟩ dumbbell[a]	⟨110⟩ dumbbell	⟨111⟩ dumbbell[a]
Mendelev	2.8553	−4.013	1.71	4.17	3.53	4.01
Dudarev	2.866	−4.316	1.97	4.48	3.64	4.13

[a] Constraint has been applied, otherwise the configuration is unstable.

The interaction energy between a point defect (N_1) and a cluster of N_{def} interstitials was estimated as

$$E_{\text{int}}^{N_{\text{def}}+N_1} = E_{\text{form}}^{N_{\text{def}}+N_1} - \left(E_{\text{form}}^{N_{\text{def}}} + E_{\text{form}}^{N_1}\right) \quad (1)$$

where $E_{\text{form}}^{N_{\text{def}}+N_1}$ is the formation energy of the system containing cluster and point defect in the configuration of interest, while $E_{\text{form}}^{N_{\text{def}}}$ and $E_{\text{form}}^{N_1}$ are the converged formation energies of a cluster and a point defect, separately calculated as

$$E_{\text{form}}^{N_{\text{def}}} = E(N_0 + N_{\text{def}}) - E_{\text{coh}} \times (N_0 + N_{\text{def}}) \quad (2)$$

where $E(N_0 + N_{\text{def}})$ is the relaxed energy of a system of N_0 atomic sites containing N_{def} defects (self-interstitials) forming a cluster and E_{coh} is the cohesive energy of the perfect crystal at the equilibrium lattice constant. (Clearly, in the case of the single vacancy $N_1 = -1$.)

3. Results

Since the long range interaction between defects occurs via interplay between their displacement fields, it is useful to recall its main features in the case of ½⟨111⟩ SIA clusters, already studied elsewhere [9] using another EP, and to extend the study to ⟨100⟩ SIA clusters. SIA clusters have platelet shapes and are composed by a collection of parallel crowdions. It is known that the main distortion of the lattice is produced within the cluster glide prism, i.e. within the prism that contains all crowdions and whose axis is parallel to the Burgers vector direction [9], which is ⟨100⟩ or ⟨111⟩ in the cases studied here. This distortion is extended over a long distance from the cluster habit plane that depends on the size of the cluster and, as will be shown, on its Burgers vector as well. The net distortion near a cluster can be attributed to the distortion from each individual defect, which is a ⟨111⟩ or a ⟨100⟩ crowdion, depending on the cluster type. The properties of each individual defect inside the cluster depend on its position in it [11], i.e. a crowdion located at the centre of the cluster will contribute to the displacement field differently from a crowdion located at the edge or somewhere in between. Local distortion also exists outside the glide prism, close to the habit plane of the cluster, in terms of an expanded region. In what follows, we show and discuss the displacement field of ⟨100⟩ and ½⟨111⟩ SIA clusters as reproduced by the applied EPs. Next we shall focus on the interaction of both types of clusters with point defects.

3.1. Displacement field of ½⟨111⟩ and ⟨100⟩ SIA clusters with different interatomic potential

The displacement field produced by a SIA loop can be characterized by the distribution of the relative interatomic distance (RID) between two adjacent atoms along the Burgers vector direction on the line perpendicular to the cluster habit plane (HP), normalized to the equilibrium distance between atoms in the perfect crystal, as has been done in [9]:

$$RID = \frac{x_K - x_{K-1} - b}{b} \quad (3)$$

where x_K and x_{K-1} are the coordinates of the two adjacent atoms along the direction of the Burgers vector of the loop and b is the modulus of the Burgers vector, coincident with the equilibrium distance between them along the chosen direction.

It is known from work done with other EPs that the distribution of the atomic displacements for a defect at the centre of the loop depends on the cluster size. For small clusters (up to a few tens of defects) the largest distortion occurs at the HP, while for larger clusters the maximum is reached a few planes away from the HP. Such a behaviour was observed for ½⟨111⟩ SIA clusters for example in [11,12]. The same effect is found with the presently used EPs and an illustration of this effect is shown in Fig. 1, where the RID distribution as a function of distance from the HP for crowdions located at the centre, middle, edge and near the edge of a ½⟨111⟩ hexagonal SIA cluster of 331 interstitials is presented, as calculated with Mendelev's potential (equivalent results where obtained with Dudarev's). Other test calculations carried out with both EPs have shown that the threshold size of the SIA cluster for this effect to be seen is between 19 and 37 interstitials.

The RID distributions estimated for ½⟨111⟩ clusters of different sizes (from 7 up to 331 interstitials) were found to be practically the same using both Dudarev's and Mendelev's EPs, for all studied positions of the crowdion along the HP. A difference between EPs was found, however, in the RID distribution of the crowdions situated on the HP at the centre and between centre and edge of ⟨100⟩ clusters. The RID distributions are plotted in Fig. 2 for crowdions located in different positions in a ⟨100⟩ SIA cluster consisting of 442 defects, calculated using both EPs. It can be seen that with Dudarev's EP the maximum of the RID for a central defect is located a few planes away from the HP (see Fig. 2(b)), similarly to the case of ½⟨111⟩ loops, while according to Mendelev's EP the maximum value is reached at the centre (see Fig. 2(a)). The absolute value of the RID at the HP was therefore found different from one potential to the other for the defects at the centre of the HP; however, exactly the same result was obtained for the defects at the edge

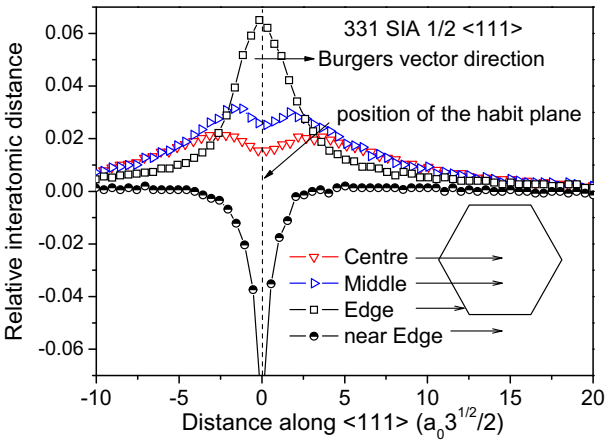

Fig. 1. The RID distribution as a function of distance from the HP for the crowdions at the centre, middle, edge and near the edge of a ½⟨111⟩ hexagonal SIA cluster consisting of 331 interstitials.

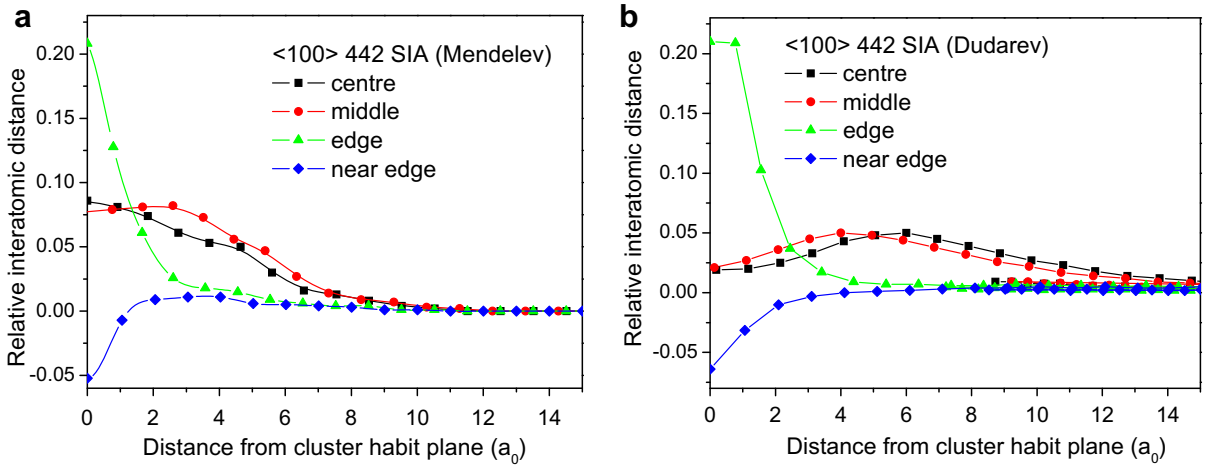

Fig. 2. Relative distance between two adjacent atoms for a ⟨100⟩ SIA cluster of 442 defects along the line perpendicular to the cluster habit plane that crosses the cluster at its centre, edge, between edge and centre (so called middle) and near edge (outside of the cluster glide prism), estimated using Mendelev's (a) and Dudarev's (b) EPs.

and in the expanded region. In Fig. 3 the RID distribution at the HP for both a ⟨100⟩ and a ½⟨111⟩ SIA cluster is illustrated in more detail as predicted by the two EPs: the comparison shows clearly that the strain field associated to the ⟨100⟩ cluster is different depending on the potential (Fig. 3(a)), though it is the same for a ½⟨111⟩ SIA cluster (Fig. 3(b)). Qualitatively it can be said that according to Dudarev's potential the displacement field associated with a ⟨100⟩ loop is more similar to the displacement field of a ½⟨111⟩ loop than according to Mendelev's potential.

3.2. Interaction between point defects and ½⟨111⟩ clusters

The interaction energies between a ½⟨111⟩ cluster of 91 SIAs and a vacancy versus distance are shown in Fig. 4(a), as estimated using Mendelev's EP. The vacancy was placed in the gliding prism of the cluster and the interaction energy was calculated after relaxation as a function of the distance from the cluster HP to the vacancy. Each curve given in the figure corresponds to the defect being located along the line passing through different crowdions of the cluster, from the centre towards the cluster edge and right outside it. The interaction is always attractive if the vacancy is inside the glide prism or just nearby its edge. The strength of the interaction (absolute value of the interaction energy) depends on the distance from defect to cluster HP and on the position of the defect in the cluster glide prism, since the RID distribution depends on it as well. The capture of a vacancy, finally leading to recombination, by this particular cluster size occurs at a distance which is less than ~6 lattice constants ($7\bullet\sqrt{3}a_0/2$, a_0 is the lattice constant) at the edge of the cluster. The recombination could also occur at the centre of the cluster, although the energy state thereby reached is much less favourable than when the recombination occurs at the edge. In intermediate position the recombination is not possible because the vacancy finds a lower energy state slightly away from the cluster HP. Thus, the recombination should occur at the edge of the cluster. This interpretation is consistent with the results obtained in Ref. [13] using a different EP. Totally equivalent results have been also obtained using Dudarev's potential.

A similar picture is found in the case of interaction between a single interstitial and a ½⟨111⟩ cluster. The main difference from the vacancy case is the existence of a quite strong repulsion when the SIA approaches the cluster within its glide prism, until a threshold distance is overcome. The only region where attraction always occurs is by the edge region (see Fig. 4(b)). This is a natural effect of the different nature of the displacement fields of the SIA (oversized object) and the vacancy (undersize object). From Fig. 4(b) it can be seen that there is a drop of the interaction energy

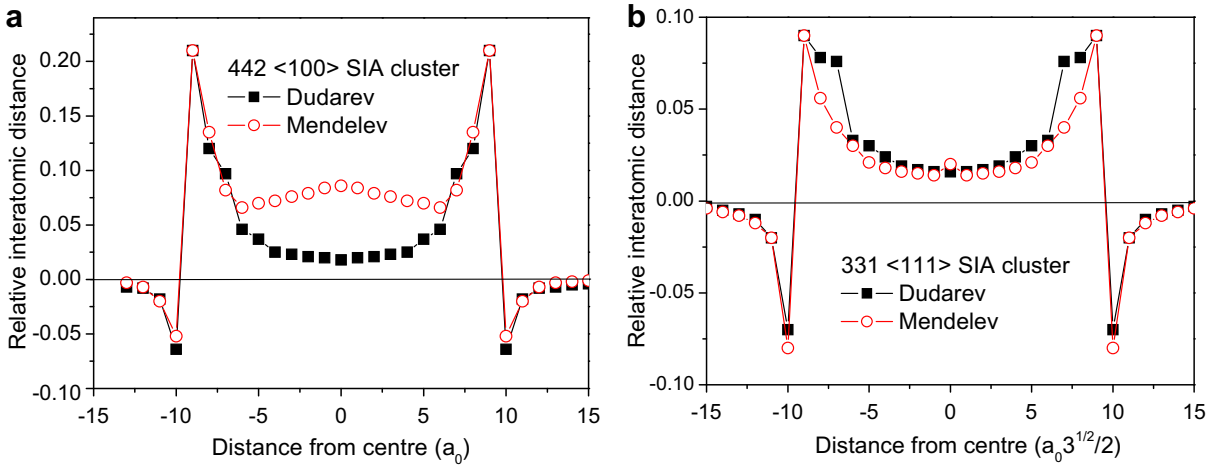

Fig. 3. Distribution of the interatomic distance between two adjacent atoms at the habit plane of a SIA cluster along the direction of the Burgers vector, as a function of the distance from the centre of the cluster, according to Mendelev's and Dudarev's EPs. (a) for a 442 ⟨100⟩ loop; (b) for a 331 ½⟨111⟩ loop.

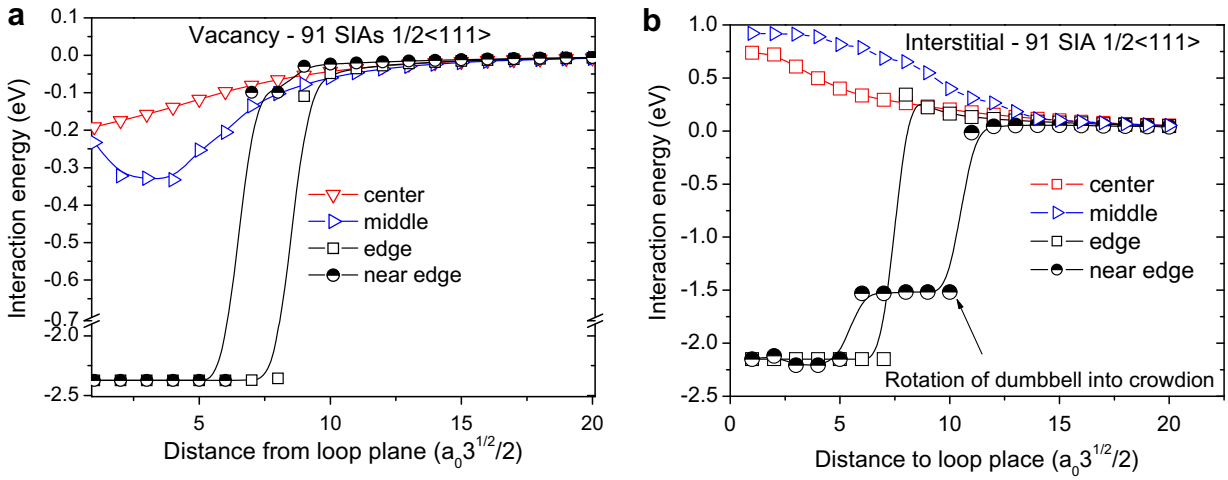

Fig. 4. Interaction energy of a ½⟨1 1 1⟩ SIA cluster consisting of 91 interstitials with a vacancy (a) and a single self-interstitial (b), as a function of distance between the defect and the cluster habit plane, when the point defect approaches the cluster along the Burgers vector direction, estimated for lines crossing the cluster at different positions, using Mendelev's EP.

at a distance of about 9 lattice units when the SIA approaches the edge of the cluster. This effect is due to the rotation of the ⟨1 1 0⟩ dumbbell into a ⟨1 1 1⟩ crowdion parallel to the crowdions in the cluster. As soon as the rotation occurs, the crowdion easily glides towards the cluster and joins it at its edge. Qualitatively and quantitatively the same interaction of single SIA with ½⟨1 1 1⟩ SIA clusters was found with Dudarev's EPs. It should be noted that the spontaneous recombination distance for an SIA (corresponding to the energy drop) is slightly longer than for a vacancy, again due to the different nature and size of the displacement fields of SIA (oversized object) and vacancy (undersize object). However, the range of attractive interaction, although very weak at the beginning, is more extended for the vacancy than for the SIA.

3.3. Interaction between point defects and ⟨1 0 0⟩ clusters

The interaction energies between a ⟨1 0 0⟩ cluster of 122 SIAs and a vacancy are shown in Fig. 5 for both EPs. Again the interaction is attractive everywhere inside the glide prism, but the lowest energy state is reached at the edge and just nearby, where recombination will occur, whereas in other positions the lowest energy state is found away from the cluster HP. The involved energy differences between vacancy locations close to the HP are, however, small, much smaller than in the case of ½⟨1 1 1⟩ loops. More importantly, this time the vacancy is captured at a distance which is less than 3 lattice constants, i.e. almost twice as small as the recombination distance found for a ½⟨1 1 1⟩ cluster of similar size (Fig. 5(a)), with Mendelev's EP. Dudarev's EP provides a somewhat larger interaction radius, close to 4 lattice constants (Fig. 5(b)), but for the rest the results are qualitatively the same and also quantitatively close to those obtained with Mendelev's EP.

The case of the interaction with a self-interstitial is illustrated in Fig. 6, where a direct comparison is made with vacancy capture for both types of loops (the curves refer to the case of point defects approaching the edge of the loop). All curves here were obtained with Mendelev's EP. It can be seen that also in the case of the SIA the absorption by a ⟨1 0 0⟩ loop occurs at a distance of 3–4 lattice units, which is again much smaller than in the case of a ½⟨1 1 1⟩ loop, as shown in the figure. Thus, ⟨1 0 0⟩ clusters clearly have a smaller capture radius for point defects. Another difference is that the dumbbell keeps its ⟨1 1 0⟩ configuration when approaching a ⟨1 0 0⟩ cluster.

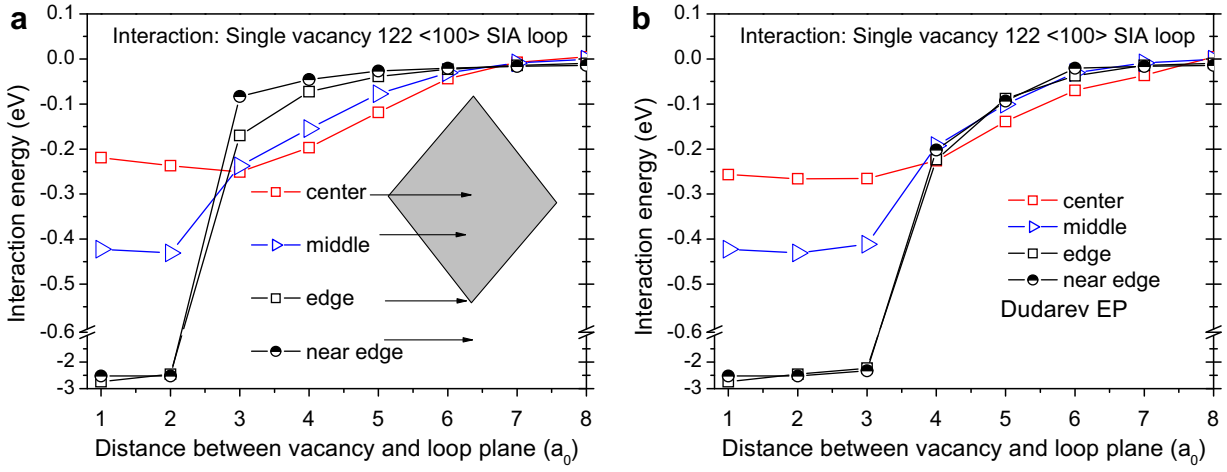

Fig. 5. Interaction energy of a ⟨1 0 0⟩ SIA cluster with a vacancy as a function of the distance between defect and cluster habit plane, when the point defect approaches the cluster along the Burgers vector direction, estimated using Mendelev's (a) and Dudarev's (b) EP.

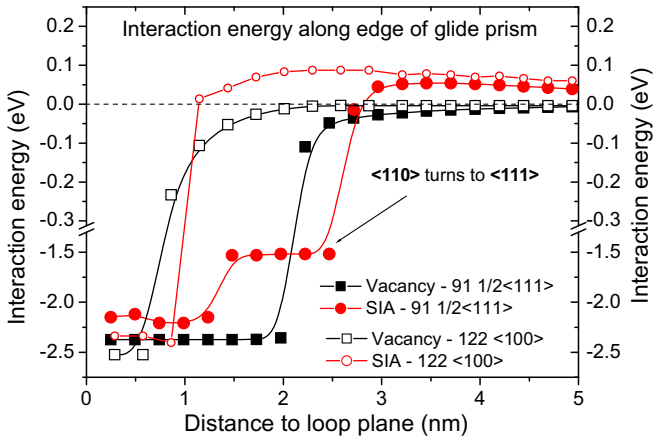

Fig. 6. Interaction energy along the edge of the glide prism between a loop and a point defect for both ½⟨111⟩ and ⟨100⟩ loops, with both SIA and vacancy, as calculated using Mendelev's EP.

Setting a numeric cut-off criterion for the interaction energy (let us take 0.05 eV, which is the order of the thermal kinetic energy of an atom at 600 K), the effective 'length' of the cluster strain field along the direction of its Burgers vector can be estimated. The results are given in Fig. 7, where this 'length' as a function of cluster size (diameter of the cluster in its HP, as schematically shown in the figure) is presented for the two used EPs. It can be seen that both applied EPs agree on that the length of the ½⟨111⟩ clusters is significantly larger then the length of ⟨100⟩ clusters having similar size. This is reflected by both EPs, although in the case of Dudarev's EP this effect is less pronounced, due to the different description of the strain field, as explained in Section 3.1.

4. Discussion

The most puzzling result obtained in the present study is that the capture radius for defects of a ½⟨111⟩ cluster is significantly larger than the capture radius of a ⟨100⟩ cluster, which is not a trivial fact. The length of the Burgers vector is normally assumed to define the extension of the displacement field around a dislocation loop and the strength of their interaction with point defects [14], therefore ⟨100⟩ clusters would be expected to have longer capture radius and stronger interaction with point defects than ½⟨111⟩ clusters. But this is not the case, if we rely on the atomistic

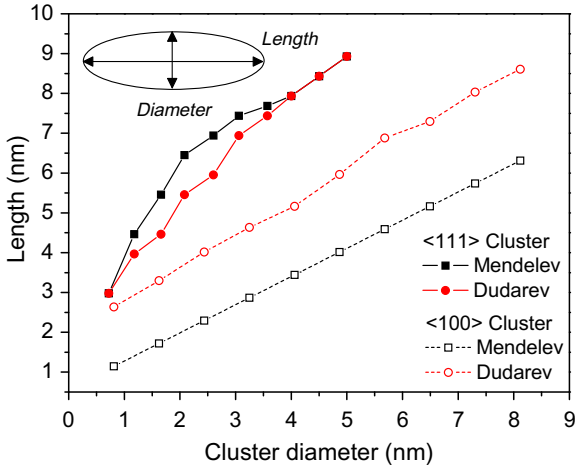

Fig. 7. The effective length of the SIA cluster versus its diameter estimated using Mendelev's and Dudarev's EPs.

studies. The origin of this may lie in the fact that in a ⟨100⟩ cluster there is a double layer of self-interstitials and this seems to reduce the anisotropy of the displacement field, compared to the ½⟨111⟩ case, via a reduction of the crowdion length inside the cluster. This reasoning seems to make sense if one compares the length of ⟨100⟩ clusters as predicted by the two different EPs and takes into account the differences in the displacement field of these clusters at the HP described in Section 3.1 (Fig. 3(a)). The origin of the longer length given by Dudarev's potential may be related to the bigger length of central ⟨100⟩ crowdions in the cluster (Fig. 2) as compared to the results provided by Mendelev's EP.

These differences in the displacement field of ⟨100⟩ clusters require further investigation to decide which potential is closer to reality, because the details of the cluster displacement field may be also related to the facility for migrating. From the simple analogy with the fast migration of ½⟨111⟩ clusters, Dudarev's EP might provide lower migration energy for a ⟨100⟩ cluster than Mendelev's EP. This aspect is going to be considered in forthcoming work, where the dynamics of cluster-defect interaction will be considered as well.

Another result of interest concerns the fact that, although the distance at which the energy interaction drop between SIA cluster and point defect occurs is larger for the absorption of an SIA than for the recombination with a vacancy, the larger range of the elastic interaction with the vacancy suggests that in practice the capture radius will be approximately the same for both point defects. The difference, however, is made by the mobility of SIA clusters, information on which is available e.g. from Ref. [15]. ½⟨111⟩ SIA clusters can absorb SIAs and vacancies with equal efficiency because: (i) they exhibit similar long range interaction with both types of point defects; (ii) they can glide with low migration barrier towards a vacancy [16] and absorb it, whereas their recombination with an SIA occurs via simultaneous fast motion of both, particularly after the transformation of the ⟨110⟩ dumbbell into a ⟨111⟩ crowdion [17]. Thus, the reaction kinetics will be governed by the mobility of the cluster, which is higher than the mobility of point defects. The ⟨100⟩ SIA clusters, on the contrary, are expected to move with much less facility than ½⟨111⟩ clusters (if they move at all). Therefore in the case of the reaction with a vacancy or a SIA, the point defect will have to move towards the cluster to be absorbed at its edge. Thus, the kinetics of the reaction will be governed by the mobility of the single defects and will be slower than in the case of ½⟨111⟩ clusters. If in addition we recall that ½⟨111⟩ clusters have longer displacement field, it appears that the net flux of point defects on these clusters should be higher than on ⟨100⟩ clusters. From the viewpoint of rate theory models it means that ½⟨111⟩ clusters should be described as sinks with preferential absorption for 3D migrating defects as compared to ⟨100⟩ clusters, something hitherto never explicitly included in existing models to our knowledge (for example [6,8,18]).

Under irradiation conditions the kinetics is governed by the interplay between several reactions whose occurrence depends on the concentration of the reactants. The evolution of the system is not intuitive. For instance in the case of two reaction channels between two reactants, depending on the (two) kinetic constants, the solution may be the disappearance of one or the other reactant, a steady state or an oscillatory behaviour. Here we have two types of loops reacting with the same flux of point defects. Because of the larger displacement field and faster mobility, the transient for ½⟨111⟩ clusters is expected to be faster than in the case of ⟨100⟩ clusters. Since they seem to be equally efficient in absorbing vacancies and SIA (and their respective clusters), the processes of growth or recombination will depend on the relative concentration of vacancies and their small 3D mobile clusters versus the concentration of SIA and their small clusters. Since at steady state the concentration of the former is expected to be higher than the

concentration of the latter, eventually ½⟨111⟩ clusters are bound to disappear, even if they fail to annihilate at sinks such as dislocations or grain boundaries. On the contrary, ⟨100⟩ loops will grow at a rate governed by the difference in fluxes of the two point defects, as well as by the flux of small 3D mobile clusters falling into their displacement field. Since the mobility of the single SIA is higher than the mobility of the single vacancy, eventually, ⟨100⟩ loops will have more chances of surviving and growing than ½⟨111⟩ loops. These considerations may thus provide a (so far) qualitative explanation for the observed ⟨100⟩-to-½⟨111⟩ concentration ratio versus dose and temperature under neutron or electron irradiation experiments, when the density of visible ⟨100⟩ loops is found to be higher than the density of ½⟨111⟩ loops, particularly with growing dose and rising temperature [3–5]. However, temperature and sink distribution are expected to play a major role on the actual microstructure evolution, which cannot be properly addressed using MD tools due to limitations in space and time scale. Further investigations and systematic application of the results in radiation-induced microstructure evolution models are therefore required to draw definitive conclusions.

5. Conclusions

1. The applied EPs provide different displacement fields at the habit plane for ⟨100⟩ clusters, and therefore different lengths of interaction of these clusters with point defects. However, the description they provide for ½⟨111⟩ clusters is very similar and both agree in predicting a more extended displacement field for these clusters than for ⟨100⟩ clusters, contrary to what should be expected based on their respective Burgers vectors.
2. Due to longer interaction distance and higher mobility, ½⟨111⟩ SIA clusters should be described as preferential and unbiased sinks for small 3D mobile defects, as compared to ⟨100⟩ clusters. Establishing further implications of these results will require further investigation using microstructure evolution models, to see if indeed they can explain the experimentally observed concentration ratio in the population of ⟨100⟩ and ½⟨111⟩ SIA loops.

Acknowledgements

This work was carried out within the framework of the Intergrated Project Eurotrans/Demetra, partially funded by the European Commission under contract FI6W-CT-2004-516520.

References

[1] G.J. Ackland, M.I. Mendelev, D.J. Srolovitz, S. Han, A.V. Barashev, J. Phys: Condens. Matter 16 (2004) 1.
[2] S. Dudarev, P. Derlet, J. Phys.: Condens. Mater. 17 (2005) 7097.
[3] N. Yoshida, J. Phys. Soc. Jpn. 39 (1975) 170.
[4] A.E. Ward, S.B. Fisher, J. Nucl. Mater. 166 (1989) 227.
[5] A.C. Nicol, M.L. Jenkins, M.A. Kirk, Mat. Res. Soc. Symp. 650 (2001) 131.
[6] A.D. Braislford, R. Bullough, J. Nucl. Mater. 69&70 (1978) 434.
[7] E.A. Little, R. Bullough, M.H. Wood, Proc. Roy. Soc. Lond. A 372 (1980) 565.
[8] R. Bullough, M.H. Wood, E.A. Little, ASTM STP 725, in: D. Kramer, H.R. Brager, J.S. Perrin (Eds.), American Society for Testing Materials, 1981, p. 593.
[9] M.A. Puigvi, Yu.N. Osetsky, A. Serra, Philos. Mag. 83 (2003) 857.
[10] C.S. Becquart, C. Domain, A. Legris, J.-C. van Duysen, J. Nucl. Mater. 280 (2000) 73.
[11] E. Kuramoto, J. Nucl. Mater. 276 (2000) 143.
[12] Yu.N. Osetsky, A. Serra, V. Priego, J. Nucl. Mater. 276 (2000) 202.
[13] M.A. Puigvi, A. Serra, N. De Diego, Yu.N. Osetsky, D.J. Bacon, Philos. Mag. Lett. 84 (2004) 257.
[14] R. Bullough, in: Proceedings of Conference 50th Anniversary of the Concept of Dislocations in Crystals, The Institute of Metals, London, 1985.
[15] Yu.N. Osetsky, D.J. Bacon, A. Serra, B.N. Singh, S.I. Golubov, Philos. Mag. A 83 (2003) 61.
[16] M. Pelfort, Yu.N. Osetsky, A. Serra, Mater. Res. Symp. 653 (2001) Z9.8.1.
[17] M. Koyanagi, K. Ohsawa, E. Kuramoto, J. Nucl. Mater. 271&272 (1999) 205.
[18] B.N. Singh, S.I. Golubov, H. Trinkaus, A. Serra, Yu.N. Osetsky, A.V. Barashev, J. Nucl. Mater. 251 (1997) 107.